Beamforming Optimization for Integrated Sensing and Communication Systems with SCNR Consideration

Eunsung Choi, Seokjun Park, Jinseok Choi, Jeonghun Park, and Namyoon Lee

***Abstract*—Integrated sensing and communication (ISAC) is acknowledged as a crucial facilitator for the advancement of future wireless communication technologies. This study introduces a combined communication and radar beamforming framework aimed at optimizing overall spectral efficiency (SE) that guarantees required radar performance, even with imperfect channel state information (CSI), in multi-user multi-target ISAC environments. To achieve this goal, we set a radar performance constraint to a receive signal-to-clutter-plus-noise ratio (SCNR) for the sum SE optimization. To address non-convexity and imperfect CSI issues, we reframe the optimization problem and derive the Karush–Kuhn–Tucker (KKT) stationarity conditions for the combined radar and communication precoding vector. By converting the condition into a nonlinear eigenvalue problem with eigenvector dependency (NEPv), we devise an alternating approach that identifies the joint precoder using power iteration and determines a Lagrangian multiplier via binary tree search. The proposed framework integrates radar and communication metrics and maintains robustness against channel estimation errors, featuring low complexity. Simulations show the effectiveness of the proposed methods.**

***Index Terms*—ISAC beamforming, imperfect CSI, receive SCNR, spectral efficiency.**

I. INTRODUCTION

The next generation of wireless communication systems aims to support high data rates, exceptional wireless connectivity to numerous devices, and robust sensing capabilities [1], [2]. To achieve these goals, the concept of integrated sensing and communication (ISAC) has been spotlighted as a key technology for future wireless systems. ISAC combines signal processing methods and hardware resources between communication and sensing systems [3]–[5]. Combining radar and communications into a single platform can lower platform costs, enable spectrum sharing, and improve performance by leveraging the synergy between radar and communication functions. Recognizing these significant benefits, we explore a multiple-input and multiple-output (MIMO) ISAC system and introduce an innovative MIMO-ISAC beamforming framework.

In early research, The ISAC system such as [6]–[9] primarily considered single-antenna systems. A crucial factor in attaining high efficiency in ISAC systems is the precise formation of multiple beams, taking into account radar targets and various communication users, which has driven the adoption of MIMO-ISAC systems. In [10], an information embedding technique was introduced, where communication signals are transmitted via MIMO radar by manipulating side lobes on a line-of-sight (LoS) environment. Furthermore, [11] proposed index-modulation type transmission methods to deliver information signals using MIMO radar waveforms.

In the context of MIMO-ISAC systems, the optimization of ISAC transmit beamforming has been extensively studied. In [12], [13], joint beamforming optimization techniques were introduced. The central concept involves using the manifold optimization technique to minimize the mean squared error (MSE) of the intended and current beampatterns while adhering to a transmit power constraint. In [12], [13], transmit symbols were utilized for both downlink user service and target sensing. However, this approach is sub-optimal compared to using designated radar sensing symbols [14]. To overcome this limitation, [15] proposed a joint beamforming optimization scheme in MIMO-ISAC systems that designates specific radar sensing symbols. A comparable issue was examined in [14], under the assumption that each communication user can cancel out radar sensing signals. [16] formulated a sum rate maximization problem, incorporating the transmit radar beam in the target angle as a penalty term, and was solved using alternating algorithms.

Preliminary research efforts on ISAC scenario have effectively highlighted the advantages of integrated systems and introduced advanced optimization techniques to improve both communication and radar performance [15], [16]. These studies have shown that shared-antenna ISAC systems outperform their separate-antenna counterparts and emphasized the benefits of using dedicated radar signals to maximize the accessible degrees of freedom (DoF). Therefore, developing ISAC beamforming methods for shared-antenna systems, particularly for imperfect CSIT cases, multi-user, and multi-target, is considered a crucial research task, which has not been fully explored. For example, [17], [18] proposed robust transmission strategies with imperfect CSIT, mainly focusing on scenarios

E. Choi, S. Park, and J. Choi are with the School of Electrical Engineering, Korea Advanced Institute of Science and Technology (KAIST), Daejeon, 34141, South Korea (e-mail: es.choi, sj.park, jinseok@kaist.ac.kr).

J. Park is with the School of Electrical and Electronic Engineering, Yonsei University, Seoul, South Korea (e-mail: jhpark@yonsei.ac.kr).

N. Lee is with the School of Electrical Engineering, Korea University, Seoul, South Korea (e-mail: namyoon@korea.ac.kr).

ISBN 978-3-903176-65-2 © 2024 IFIP

with a single user or a single target. Several previous works have addressed multi-user [15], [16] and multi-target cases [15]. However, [15], [16] primarily assumed a CSIT is perfect. To overcome this issue, we propose a robust framework of joint communication and radar beamforming, utilizing dedicated radar signals in ISAC systems in the presence of multi-user and multi-target, considering the imperfect CSIT.

In this paper, we introduce a robust comprehensive joint optimization framework in MIMO-ISAC systems, aiming to maximize the sum spectral efficiency (SE) while satisfying the required radar performances. The proposed method considers imperfect CSIT for multiple users and multiple targets, incorporating radar metrics with constucted radar signals. Our contributions are summarized as follows:

- We formulate ISAC beamforming problems that maximize the sum SE while considering the radar signal-to-clutter-plus-noise ratio (SCNR). Formulated problems incorporate both transmit and receive aspects of radar signals. The challenges arise from the non-convexity and imperfect CSIT. To address this, we propose a robust joint optimization framework.
- We derive a lower bound on the average SE based on channel estimation error, allowing us to use the error covariance in optimization. The problems are reformulated by expressing the objective function and its constraints as functions of a vectorized joint communication and radar precoder. We then establish the Lagrangian function and derive the Karush–Kuhn–Tucker (KKT) condition to search stationary points for a given Lagrangian multiplier.
- We recognize the KKT stationarity condition as a non-linear eigenvalue problem (NEPv) with eigenvector dependency, where the principal eigenvector corresponds to the best stationary point. We propose a generalized power iteration (GPI)-based algorithm to compute eigenvector. Then, a binary search algorithm updates the Lagrangian multiplier to meet the SCNR constraint, with both the precoding vector and the Lagrangian multiplier computed alternately until convergence. We also propose radar-only beam design algorithms as a special case.
- Simulations show that our proposed algorithms outperform benchmarks, providing a good trade-off between radar and communication performance and robustness for imperfect CSIT cases. Additionally, our method provides crucial design guidelines for MIMO-ISAC, highlighting the significance of the proposed robust optimization framework.

Notation: Here, a is a scalar, $\mathbf{a}$ is a vector, and $\mathbf{A}$ is a matrix. Superscripts $(\cdot)^{-1}$, $(\cdot)^{\mathsf{T}}$, and $(\cdot)^{\mathsf{H}}$ denote matrix inversion, Hermitian, and transpose, respectively. $\mathbb{E}[\cdot]$ represents expectation, and $\mathrm{tr}(\cdot)$ denotes the trace of a matrix. $\mathbf{I}_N$ is the $N{\times}N$ identity matrix, and $\mathbf{0}_{N\times M}$ is the $N{\times}M$ zero matrix. The Kronecker product is denoted by $\otimes$, and $\mathbf{e}_n^N$ is an $N{\times}1$ standard basis vector with the nth element equal to one. $\mathrm{diag}(\mathbf{a})$ is a diagonal matrix with $\mathbf{a}$ on its diagonal elements. $\mathcal{CN}(m,\sigma^2)$ denotes a complex Gaussian distribution with mean m and variance σ^2.

II. System Model

A. Signal Model

A MIMO-ISAC system is considered where the base station (BS) is equipped with an ISAC transmit antenna and a radar receive antenna on an integrated hardware platform. BS has N transmit and receive antennas, serving K single-antenna communication users and generating radar beam patterns to detect radar targets. The ISAC BS shares the same time resources, frequency resources, and transmit antenna arrays. Following the assumption in [9], we ensure full decoupling between transmit antennas and receive antennas to prevent self-interference at the received radar signal. To fully utilize the spatial degrees of freedom (DoF) from the MIMO system, the BS superimposes dedicated radar signals with communication symbols. Thus, the transmit signal $\mathbf{x} \in \mathbb{C}^N$ from the BS defined as

$$\mathbf{x} = \mathbf{F}_{\mathrm{C}}\mathbf{s}_{\mathrm{C}} + \mathbf{F}_{\mathrm{R}}\mathbf{s}_{\mathrm{R}} = [\mathbf{F}_{\mathrm{C}}, \mathbf{F}_{\mathrm{R}}]\left[\mathbf{s}_{\mathrm{C}}^{\mathsf{T}}, \mathbf{s}_{\mathrm{R}}^{\mathsf{T}}\right]^{\mathsf{T}} = \mathbf{F}\mathbf{s}, \tag{1}$$

where $\mathbf{s}_{\mathrm{C}} = [s_{\mathrm{C},1}, \ldots, s_{\mathrm{C},K}]^{\mathsf{T}} \in \mathbb{C}^K$ is a communication message symbol vector, $\mathbf{s}_{\mathrm{R}} = [s_{\mathrm{R},1}, \ldots, s_{\mathrm{R},K}]^{\mathsf{T}} \in \mathbb{C}^M$ is a radar waveform signal vector, $\mathbf{F}_{\mathrm{C}} = \left[\mathbf{f}_{\mathrm{C},1}, \cdots, \mathbf{f}_{\mathrm{C},K}\right] \in \mathbb{C}^{N\times K}$ is a communication beamforming matrix, and $\mathbf{F}_{\mathrm{R}} = \left[\mathbf{f}_{\mathrm{R},1}, \cdots, \mathbf{f}_{\mathrm{R},M}\right] \in \mathbb{C}^{N\times M}$ is a radar beamforming matrix.

As an assumption, the communication symbols $\mathbf{s}_{\mathrm{C}}$ and the radar waveform signal $\mathbf{s}_{\mathrm{R}}$ are zero-mean and statistically independent to each other, i.e., $\mathbb{E}\left[\mathbf{s}_{\mathrm{R}}\mathbf{s}_{\mathrm{C}}^{\mathsf{H}}\right] = \mathbf{0}_{M\times K}$, with $\mathbb{E}\left[\mathbf{s}_{\mathrm{R}}\mathbf{s}_{\mathrm{R}}^{\mathsf{H}}\right] = P \cdot \mathbf{I}_M$, and $\mathbb{E}\left[\mathbf{s}_{\mathrm{C}}\mathbf{s}_{\mathrm{C}}^{\mathsf{H}}\right] = P \cdot \mathbf{I}_K$, where P is the transmit power. We assume $\|\mathbf{F}_{\mathrm{R}}\|_{\mathsf{F}} + \|\mathbf{F}_{\mathrm{C}}\|_{\mathsf{F}} \leq 1$ without loss of generality to satisty a transmit power constraint.

B. Channel Model

Considering communication users, the k-th users' received signal y_k is

$$y_k = \mathbf{h}_k^{\mathsf{H}}\mathbf{f}_{\mathrm{C},k}s_{\mathrm{C},k} + \sum_{i\neq k, i=1}^{K} \mathbf{h}_k^{\mathsf{H}}\mathbf{f}_{\mathrm{C},i}s_{\mathrm{C},i} + \sum_{j=1}^{M} \mathbf{h}_k^{\mathsf{H}}\mathbf{f}_{\mathrm{R},j}s_{\mathrm{R},j} + n_k, \tag{2}$$

where $\mathbf{h}_k \in \mathbb{C}^N$ is the channel vector of k-th user, and $n_k \sim \mathcal{CN}(0, \sigma^2)$ is the additive white Gaussian noise (AWGN). In (2), the second component represents the combined interference of other users' signals, while the third component represents the combined interference of the radar signals.

We assume that each channel vector $\mathbf{h}_k \sim \mathcal{CN}(\mathbf{0}_{K\times 1}, \mathbf{K}_k)$, indicating it follows a Gaussian distribution characterized by a particular spatial covariance matrix $\mathbf{K}_k$. Based on this model, $\mathbf{h}_k$ is expressed as

$$\mathbf{h}_k = \mathbf{U}_k\mathbf{\Lambda}_k^{\frac{1}{2}}\tilde{\mathbf{h}}_k, \tag{3}$$

where $\tilde{\mathbf{h}}_k \in \mathbb{C}^{r_k}$ is an independent and identically distributed (IID) channel vector with elements which follows $\mathcal{CN}(0,1)$. $\mathbf{U}_k \in \mathbb{C}^{N\times r_k}$ comprises the eigenvectors of $\mathbf{K}_k$ associated with

$\mathbf{\Lambda}_k$, and $\mathbf{\Lambda}_k \in \mathbb{C}^{r_k \times r_k}$ is a diagonal matrix containing the non-zero eigenvalues of $\mathbf{K}_k$. It is worth noting that the channel model in (3) involves the majority of generally applied models of spatially correlated MIMO channel.

Taking into account imperfect CSIT, the estimated channel vector $\hat{\mathbf{h}}_k$ is

$$\hat{\mathbf{h}}_k = \mathbf{h}_k - \boldsymbol{\phi}_k, \tag{4}$$

where $\boldsymbol{\phi}_k$ is the channel estimation error. As an assumption, $\hat{\mathbf{h}}_k$ and $\boldsymbol{\phi}_k$ follow Gaussian distribution and independent of each other. Here, $\mathbf{\Phi}_k = \mathbb{E}[\boldsymbol{\phi}_k \boldsymbol{\phi}_k^{\mathsf{H}}]$ is the error covariance. We assume that the BS know both $\hat{\mathbf{h}}_k$ and $\mathbf{\Phi}_k$.

C. Radar Model

Effective sensing often requires a line-of-sight (LoS) path between the target and the sensor object. Compared to communication systems, which exploit multiple channel paths for better performance, clutter in radar systems degrades sensing accuracy and must be mitigated. Considering clutter referring to [2], the received radar echo signal is expressed as

$$\begin{aligned}\mathbf{y}_{\mathrm{R}} &= \sum_{i=1}^{S} \beta_i^{\mathrm{tar}} \mathbf{a}_{\mathrm{r}}(\theta_i^{\mathrm{tar}}) \mathbf{a}_{\mathrm{t}}^{\mathsf{H}}(\theta_i^{\mathrm{tar}}) \mathbf{x} + \sum_{j=1}^{C} \beta_j^{\mathrm{cl}} \mathbf{a}_{\mathrm{r}}(\theta_j^{\mathrm{cl}}) \mathbf{a}_{\mathrm{t}}^{\mathsf{H}}(\theta_j^{\mathrm{cl}}) \mathbf{x} + \mathbf{n}_{\mathrm{R}} \\ &= \mathbf{G}_{\mathrm{tar}} \mathbf{x} + \mathbf{G}_{\mathrm{cl}} \mathbf{x} + \mathbf{n}_{\mathrm{R}},\end{aligned} \tag{5}$$

where S, C, $\mathbf{a}_{\mathrm{t}}(\theta)$, and $\mathbf{a}_{\mathrm{r}}(\theta)$ are the number of targets, the number of clutters, the transmit array response vector from θ, and the receiver array response vector from θ, respectively. We denote θ_i^{tar} as the direction of the i-th target, θ_j^{cl} as the direction of the j-th clutter, β_i^{tar} as the reflection coefficient of the i-th target, and β_j^{cl} as the reflection coefficient of the j-th clutter. $\mathbf{n}_{\mathrm{R}} \sim \mathcal{CN}(\mathbf{0}_{N\times 1}, \sigma_{\mathrm{R}}^2 \mathbf{I}_N)$ as the AWGN noise. Also, $\mathbf{G}_{\mathrm{tar}} = \sum_{i=1}^{S} \beta_i^{\mathrm{tar}} \mathbf{a}_{\mathrm{r}}(\theta_i^{\mathrm{tar}}) \mathbf{a}_{\mathrm{t}}^{\mathsf{H}}(\theta_i^{\mathrm{tar}})$ and $\mathbf{G}_{\mathrm{cl}} = \sum_{j=1}^{C} \beta_j^{\mathrm{cl}} \mathbf{a}_{\mathrm{r}}(\theta_j^{\mathrm{cl}}) \mathbf{a}_{\mathrm{t}}^{\mathsf{H}}(\theta_j^{\mathrm{cl}})$. As an assumption, the reflection coefficients and directions of both clutters and targets are known at the BS, as these are large-scale parameters. Furthermore, if clutters are stationary objects, θ_j^{cl} and β_j^{cl} remain nearly time-invariant. We note that the aforementioned model can be considered as representing a subcarrier of an OFDM system or narrowband system.

D. Performance Metrics and Problem Formulation

1) Metric of Communication Performance: As a performance metric of communication, we adopt a sum SE. Firstly, the SINR at k-th user is

$$\gamma_k = \frac{\left|\mathbf{h}_k^{\mathsf{H}} \mathbf{f}_{\mathrm{C},k}\right|^2}{\sum_{i\neq k, i=1}^{K} \left|\mathbf{h}_k^{\mathsf{H}} \mathbf{f}_{\mathrm{C},i}\right|^2 + \sum_{j=1}^{M} \left|\mathbf{h}_k^{\mathsf{H}} \mathbf{f}_{\mathrm{R},j}\right|^2 + \frac{\sigma^2}{P}}. \tag{6}$$

In (6), the denominator term contains the inter-user interference and the radar waveform interference. Further, the k-th users' achieved SE is

$$R_k = \log_2 (1 + \gamma_k). \tag{7}$$

2) Radar Performance Metric: SCNR serves as a useful metric for radar performance when non-negligible clutters coexist. For example, the SCNR metric is effective during the radar tracking phase, where expected target positions and clutter locations are known. Based on [2], [19], the SCNR is computed from (5) as

$$\gamma_{\mathrm{R}}(\mathbf{F}) = \frac{\mathbb{E}[\|\mathbf{G}_{\mathrm{tar}}\mathbf{x}\|_{\mathsf{F}}]}{\mathbb{E}[\|\mathbf{G}_{\mathrm{cl}}\mathbf{x}\|_{\mathsf{F}} + \|\mathbf{n}_{\mathrm{R}}\|_{\mathsf{F}}]} = \frac{\mathrm{Tr}\left(\mathbf{G}_{\mathrm{tar}}\mathbf{F}\mathbf{F}^{\mathsf{H}}\mathbf{G}_{\mathrm{tar}}^{\mathsf{H}}\right)}{\mathrm{Tr}\left(\mathbf{G}_{\mathrm{cl}}\mathbf{F}\mathbf{F}^{\mathsf{H}}\mathbf{G}_{\mathrm{cl}}^{\mathsf{H}}\right) + \frac{N}{P}\sigma_{\mathrm{R}}^2}. \tag{8}$$

Utilizing SCNR as defined in (8) accounts for the impact of clutters, but direct beam pattern design cannot be performed.

3) Problem Formulation: The primary design objective is to maximize the sum SE satisfying the condition that the receive SCNR is smaller than the predefined threshold T_{scnr}, considering communication-oriented ISAC systems.

$$\underset{\mathbf{F}}{\text{maximize}} \quad R_{\Sigma}(\mathbf{F}) = \sum_{k=1}^{K} R_k(\mathbf{F}) \tag{9}$$

$$\text{subject to} \quad \gamma_{\mathrm{R}}(\mathbf{F}) \geq T_{\mathrm{scnr}}, \tag{10}$$

$$\mathrm{Tr}(\mathbf{F}\mathbf{F}^{\mathsf{H}}) \leq 1, \tag{11}$$

where (11) is the total transmit power constraint. Because of the non-convexity of the problem (9), the sum SE R_{Σ} must be addressed to entirely exploit the estimated channel and channel error covariance under the imperfect CSIT.

III. Proposed Optimization Framework

In this section, we present our comprehensive framework to address the problem stated in (9). Initially, we reformulate (9) into more tractable form. Utilizing this reformulation, we then examine the KKT stationary condition and propose a robust algorithm to compute the best staitionary point.

A. Problem Reformulation

Under an imperfect CSIT scenario, the estimated CSIT $\hat{\mathbf{h}}_k$ and error covariance matrix $\mathbf{\Phi}_k$ are only available at the BS. Consequently, we need to obtain a proper objective function instead of $R_{\Sigma}(\mathbf{F})$. Therefore, we take into account the average SE concerning the CSIT estimation error [20] as

$$\begin{aligned}\bar{R}_k(\mathbf{F}) &= \mathbb{E}_{\boldsymbol{\phi}_k}[R_k(\mathbf{F})] \\ &= \mathbb{E}_{\boldsymbol{\phi}_k}\left[\log_2\left(1 + \frac{\left|\left(\hat{\mathbf{h}}_k + \boldsymbol{\phi}_k\right)^{\mathsf{H}} \mathbf{f}_{\mathrm{C},k}\right|^2}{\sum_{i\neq k}^{K} \left|\left(\hat{\mathbf{h}}_k + \boldsymbol{\phi}_k\right)^{\mathsf{H}} \mathbf{f}_{\mathrm{C},i}\right|^2 + \sum_{j=1}^{M} \left|\left(\hat{\mathbf{h}}_k + \boldsymbol{\phi}_k\right)^{\mathsf{H}} \mathbf{f}_{\mathrm{C},j}\right|^2 + \frac{\sigma^2}{P}}\right)\right].\end{aligned} \tag{12}$$

to obtain a proper SE expression, we rewrite (2) with the CSIT estimation error as

$$\begin{aligned} y_k = {} & \hat{\mathbf{h}}_k^{\mathsf{H}} \mathbf{f}_{\mathrm{C},k} s_{\mathrm{C},k} + \sum_{i\neq k, i=1}^{K} \hat{\mathbf{h}}_k^{\mathsf{H}} \mathbf{f}_{\mathrm{C},i} s_{\mathrm{C},i} + \sum_{j=1}^{M} \hat{\mathbf{h}}_k^{\mathsf{H}} \mathbf{f}_{\mathrm{R},j} s_{\mathrm{R},j} \\ & + \underbrace{\sum_{i'=1}^{K} \boldsymbol{\phi}_k^{\mathsf{H}} \mathbf{f}_{\mathrm{C},i'} s_{\mathrm{C},i'} + \sum_{j'=1}^{M} \boldsymbol{\phi}_k^{\mathsf{H}} \mathbf{f}_{\mathrm{R},j'} s_{\mathrm{R},j'} + n_k}_{(a)}. \end{aligned} \tag{16}$$

$$\bar{R}_k(\mathbf{F}) \geq \mathbb{E}_{\boldsymbol{\phi}_k}\left[\log_2\left(1+\frac{\left|\hat{\mathbf{h}}_k^{\mathsf{H}}\mathbf{f}_{\mathrm{C},k}\right|^2}{\sum_{i\neq k,i=1}^{K}\left|\hat{\mathbf{h}}_k^{\mathsf{H}}\mathbf{f}_{\mathrm{C},i}\right|^2+\sum_{j=1}^{M}\left|\hat{\mathbf{h}}_k^{\mathsf{H}}\mathbf{f}_{\mathrm{R},j}\right|^2+\sum_{i'=1}^{K}\left|\boldsymbol{\phi}_k^{\mathsf{H}}\mathbf{f}_{\mathrm{C},i'}\right|^2+\sum_{j'=1}^{M}\left|\boldsymbol{\phi}_k^{\mathsf{H}}\mathbf{f}_{\mathrm{R},j'}\right|^2+\frac{\sigma^2}{P}}\right)\right] \tag{13}$$

$$\overset{(b)}{\geq} \log_2\left(1+\frac{\left|\hat{\mathbf{h}}_k^{\mathsf{H}}\mathbf{f}_{\mathrm{C},k}\right|^2}{\sum_{i\neq k,i=1}^{K}\left|\hat{\mathbf{h}}_k^{\mathsf{H}}\mathbf{f}_{\mathrm{C},i}\right|^2+\sum_{j=1}^{M}\left|\hat{\mathbf{h}}_k^{\mathsf{H}}\mathbf{f}_{\mathrm{R},j}\right|^2+\sum_{i'=1}^{K}\mathbf{f}_{\mathrm{C},i'}^{\mathsf{H}}\boldsymbol{\Phi}_k\mathbf{f}_{\mathrm{C},i'}+\sum_{j'=1}^{M}\mathbf{f}_{\mathrm{R},j'}^{\mathsf{H}}\boldsymbol{\Phi}_k\mathbf{f}_{\mathrm{R},j'}+\frac{\sigma^2}{P}}\right) \tag{14}$$

$$= \bar{R}_k^{\mathsf{lb}}(\mathbf{F}). \tag{15}$$

We note that the term (a) involves some randomness related to $\boldsymbol{\phi}_k$, $\mathbf{s}_{\mathrm{C}}$, and $\mathbf{s}_{\mathrm{R}}$. Even though (a) is correlated with the intended signal term because of $\mathbf{s}_{\mathrm{C},k}$, we eliminate the correlation by regarding (a) as an independent Gaussian interference. By applying the notion of generalized mutual information in [21], this assumption results in a lower bound of the SE R_k. Then, the following lower bound of (12) as presented in (15) at the top of the page where (b) is derived using Jensen's inequality and $\mathbb{E}[\boldsymbol{\phi}_k\boldsymbol{\phi}_k^{\mathsf{H}}] = \boldsymbol{\Phi}_k$. With the derived closed-form, we define $\bar{R}_k^{\mathsf{lb}}$ for a new objective function. We note that $\bar{R}_k^{\mathsf{lb}}$ is a function of $\hat{\mathbf{h}}_k$ and $\boldsymbol{\Phi}_k$ which are available at the BS. We denote the vectorized beamforming variable as $\bar{\mathbf{f}} = \mathrm{vec}(\mathbf{F}) \in \mathbb{C}^{N(K+M)}$. Also, we assume maximum transmit power P, i.e., $\|\bar{\mathbf{f}}\|^2 = 1$. To this end, for more tractability, we reconstruct $\bar{R}_k^{\mathsf{lb}}$ as

$$\bar{R}_k^{\mathsf{lb}}(\bar{\mathbf{f}}) = \log_2\left(\frac{\bar{\mathbf{f}}^{\mathsf{H}}\mathbf{B}_k\bar{\mathbf{f}}}{\bar{\mathbf{f}}^{\mathsf{H}}\mathbf{C}_k\bar{\mathbf{f}}}\right), \tag{17}$$

where $\mathbf{B}_k = \mathbf{I}_{(K+M)} \otimes \left(\hat{\mathbf{h}}_k\hat{\mathbf{h}}_k^{\mathsf{H}}+\boldsymbol{\Phi}_k\right)+\frac{\sigma^2}{P}\mathbf{I}_{N(K+M)}$ and $\mathbf{C}_k = \mathbf{B}_k - \mathrm{diag}\left(\mathbf{e}_k^{(K+M)}\right)\otimes\hat{\mathbf{h}}_k\hat{\mathbf{h}}_k^{\mathsf{H}}$.

Now, we reformulate the SCNR constraint as a function of $\bar{\mathbf{f}}$. We rewrite the SCNR in (8) as

$$\gamma_{\mathrm{R}} = \frac{\mathrm{vec}(\mathbf{G}_{\mathrm{tar}}\mathbf{F})^{\mathsf{H}}\mathrm{vec}(\mathbf{G}_{\mathrm{tar}}\mathbf{F})}{\mathrm{vec}(\mathbf{G}_{\mathrm{cl}}\mathbf{F})^{\mathsf{H}}\mathrm{vec}(\mathbf{G}_{\mathrm{cl}}\mathbf{F})+\frac{N}{P}\sigma_{\mathrm{R}}^2} \tag{18}$$

$$\overset{(a)}{=} \frac{\bar{\mathbf{f}}^{\mathsf{H}}(\mathbf{I}_{K+M}\otimes\mathbf{G}_{\mathrm{tar}})^{\mathsf{H}}(\mathbf{I}_{K+M}\otimes\mathbf{G}_{\mathrm{tar}})\bar{\mathbf{f}}}{\bar{\mathbf{f}}^{\mathsf{H}}(\mathbf{I}_{K+M}\otimes\mathbf{G}_{\mathrm{cl}})^{\mathsf{H}}(\mathbf{I}_{K+M}\otimes\mathbf{G}_{\mathrm{cl}})\bar{\mathbf{f}}+\frac{N}{P}\sigma_{\mathrm{R}}^2}, \tag{19}$$

where (a) is derived by $\mathrm{vec}(\mathbf{ABC}) = (\mathbf{C}^{\mathsf{T}}\otimes\mathbf{A})\mathrm{vec}(\mathbf{B})$.

Under assumption of maximum transmit power, i.e., $\|\bar{\mathbf{f}}\|^2 = 1$, (19) is reformulated as

$$\mathrm{SCNR}_{\mathrm{R}}(\mathbf{F}) = \frac{\bar{\mathbf{f}}^{\mathsf{H}}\bar{\mathbf{G}}_{\mathrm{tar}}\bar{\mathbf{f}}}{\bar{\mathbf{f}}^{\mathsf{H}}\bar{\mathbf{G}}_{\mathrm{cl}}\bar{\mathbf{f}}}, \tag{20}$$

where

$$\bar{\mathbf{G}}_{\mathrm{tar}} = (\mathbf{I}_{K+M}\otimes\mathbf{G}_{\mathrm{tar}})^{\mathsf{H}}(\mathbf{I}_{K+M}\otimes\mathbf{G}_{\mathrm{tar}}), \tag{21}$$

$$\bar{\mathbf{G}}_{\mathrm{cl}} = (\mathbf{I}_{K+M}\otimes\mathbf{G}_{\mathrm{cl}})^{\mathsf{H}}(\mathbf{I}_{K+M}\otimes\mathbf{G}_{\mathrm{cl}})+\frac{N}{P}\sigma_{\mathrm{R}}^2\mathbf{I}_{N(K+M)}. \tag{22}$$

Lastly, we omit the power constraint $\mathrm{Tr}(\mathbf{F}\mathbf{F}^{\mathsf{H}}) = \|\bar{\mathbf{f}}\|^2 = 1$ to relax the problem and regard it in the algorithm to obtain a solution within a feasible set. Substituting (17) and (20) to the problem of (9) reconstructs the main problem as

$$\underset{\bar{\mathbf{f}}}{\text{maximize}} \quad \bar{R}_{\Sigma}^{\mathsf{lb}}(\bar{\mathbf{f}}) \tag{23}$$

$$\text{subject to} \quad \frac{\bar{\mathbf{f}}^{\mathsf{H}}\bar{\mathbf{G}}_{\mathrm{tar}}\bar{\mathbf{f}}}{\bar{\mathbf{f}}^{\mathsf{H}}\bar{\mathbf{G}}_{\mathrm{cl}}\bar{\mathbf{f}}} \geq T_{\mathrm{scnr}}. \tag{24}$$

Since the reconstructed problem (23) is still non-convex, it is an NP-hard problem to search a global optimal solution. Therefore, we adopt a GPI-based algorithm to find the best stationary solution of the reconstructed problem (23).

B. Proposed GPI-ISAC-SCNR Algorithm

To find a stationary point, we derive the KKT stationarity condition of (23) as follows.

Lemma 1. *The first-order KKT condition of* (23) *is fulfilled if the following condition holds:*

$$\boldsymbol{\Psi}(\bar{\mathbf{f}})\bar{\mathbf{f}} = \boldsymbol{\Omega}(\bar{\mathbf{f}})\lambda(\bar{\mathbf{f}})\bar{\mathbf{f}}, \tag{25}$$

where

$$\boldsymbol{\Psi}(\bar{\mathbf{f}}) = \lambda_{\mathsf{num}}(\bar{\mathbf{f}})\left(\sum_{k=1}^{K}\frac{\mathbf{B}_k}{\bar{\mathbf{f}}^{\mathsf{H}}\mathbf{B}_k\bar{\mathbf{f}}}+\mu\frac{\bar{\mathbf{G}}_{\mathrm{tar}}}{\bar{\mathbf{f}}^{\mathsf{H}}\bar{\mathbf{G}}_{\mathrm{tar}}\bar{\mathbf{f}}}\right), \tag{26}$$

$$\boldsymbol{\Omega}(\bar{\mathbf{f}}) = \lambda_{\mathsf{den}}(\bar{\mathbf{f}})\left(\sum_{k=1}^{K}\frac{\mathbf{C}_k}{\bar{\mathbf{f}}^{\mathsf{H}}\mathbf{C}_k\bar{\mathbf{f}}}+\mu\frac{\bar{\mathbf{G}}_{\mathrm{cl}}}{\bar{\mathbf{f}}^{\mathsf{H}}\bar{\mathbf{G}}_{\mathrm{cl}}\bar{\mathbf{f}}}\right). \tag{27}$$

Here, μ *in* (26) *and* (27) *is the Lagrangian multiplier and*

$$\lambda(\bar{\mathbf{f}}) = T_{\mathrm{scnr}}^{-\mu}\left(\frac{\bar{\mathbf{f}}^{\mathsf{H}}\bar{\mathbf{G}}_{\mathrm{tar}}\bar{\mathbf{f}}}{\bar{\mathbf{f}}^{\mathsf{H}}\bar{\mathbf{G}}_{\mathrm{cl}}\bar{\mathbf{f}}}\right)^{\mu}\prod_{k=1}^{K}\left(\frac{\bar{\mathbf{f}}^{\mathsf{H}}\mathbf{B}_k\bar{\mathbf{f}}}{\bar{\mathbf{f}}^{\mathsf{H}}\mathbf{C}_k\bar{\mathbf{f}}}\right) = \frac{\lambda_{\mathsf{num}}(\bar{\mathbf{f}})}{\lambda_{\mathsf{den}}(\bar{\mathbf{f}})}. \tag{28}$$

where $\lambda_{\mathsf{num}}(\bar{\mathbf{f}})$ *and* $\lambda_{\mathsf{den}}(\bar{\mathbf{f}})$ *are any functions that meet the condition of* (28).

Proof. See Appendix A. ∎

However, since the reformulated problem (23) is non-convex, searching a global optimal point using the derived condition is infeasible, and only the necessary condition for a local optimal point can be ensured. Furthermore, the Lagrangian multiplier μ and the optimization variable $\bar{\mathbf{f}}$ are intricately interdependent, making their joint optimization challenging. To address this issue, we alternately optimize μ and $\bar{\mathbf{f}}$ based on Lemma 1 to find the best local optimal solution.

We note that when $\bar{\mathbf{f}}$ satisfies (25), then it meets the first-order optimality condition. To find best local optimal solution, we describe relationship between the objective function $\bar{R}_{\Sigma}^{\mathsf{lb}}(\bar{\mathbf{f}})$

Algorithm 1: GPI-based precoding

initialize: $\bar{\mathbf{f}}_{(0)}$
Set $t = 1$.
while $\left\|\bar{\mathbf{f}}_{(t)} - \bar{\mathbf{f}}_{(t-1)}\right\| > \epsilon$ *or* $t < t_{\max}$ **do**
  Compute matrix $\mathbf{\Psi}(\bar{\mathbf{f}}_{(t-1)})$ according to (26).
  Compute matrix $\mathbf{\Omega}(\bar{\mathbf{f}}_{(t-1)})$ according to (27).
  Update $\bar{\mathbf{f}}_{(t)} \leftarrow \frac{\mathbf{\Omega}^{-1}(\bar{\mathbf{f}}_{(t-1)})\mathbf{\Psi}(\bar{\mathbf{f}}_{(t-1)})\bar{\mathbf{f}}_{(t-1)}}{\|\mathbf{\Omega}^{-1}(\bar{\mathbf{f}}_{(t-1)})\mathbf{\Psi}(\bar{\mathbf{f}}_{(t-1)})\bar{\mathbf{f}}_{(t-1)}\|}$.
  $t \leftarrow t + 1$.
$\bar{\mathbf{f}} \leftarrow \bar{\mathbf{f}}_{(t)}$
return $\bar{\mathbf{f}}$.

Algorithm 2: GPI-ISAC-SCNR

initialize: $\mu_{(1)} = \mu_{\max}$.
Set the iteration count $n = 1$ and
while $|\mu_{(n)} - \mu_{(n-1)}| > \zeta$ *or* $n \le n_{\max}$ **do**
  $\bar{\mathbf{f}} \leftarrow$ Algorithm 1 with $\mu_{(n)}$
  if $T_{\text{scnr}} < \frac{\mathrm{Tr}\left(\mathbf{G}_{\text{tar}}\mathbf{F}\mathbf{F}^{\mathsf{H}}\mathbf{G}_{\text{tar}}^{\mathsf{H}}\right)}{\mathrm{Tr}\left(\mathbf{G}_{\text{cl}}\mathbf{F}\mathbf{F}^{\mathsf{H}}\mathbf{G}_{\text{cl}}^{\mathsf{H}}\right)+\frac{N}{P}\sigma_{\text{R}}^2}$ **then**
    $\mu_{(n+1)} \leftarrow (\mu_{(n)} + \mu_{\min})/2$
  else
    $\mu_{(n+1)} \leftarrow (\mu_{(n)} + \mu_{\max})/2$
  $n \leftarrow n + 1$.
$\bar{\mathbf{f}}^\star \leftarrow \bar{\mathbf{f}}$
return $\bar{\mathbf{f}}^\star$

in (23) and $\lambda(\bar{\mathbf{f}})$ in (25). As an assumption, we have an arbitrary pair of precoder and Lagrangian multiplier $(\bar{\mathbf{f}}^\dagger, \mu^\dagger)$ that meets the SCNR constraint (24) with equality and the first-order optimality condition (25). In such a case, we have $\log_2 \lambda(\bar{\mathbf{f}}^\dagger) = R_\Sigma^{\text{lb}}(\bar{\mathbf{f}}^\dagger)$ which is a stationary point from the first-order optimality condition because of the active SCNR constraint. Therefore, we then have to find $(\bar{\mathbf{f}}^\dagger, \mu^\dagger)$ which maximizes $\lambda(\bar{\mathbf{f}}^\dagger)$.

To find the best local optimal point, we regard (25) as a functional eigenvalue problem. Since $\mathbf{\Omega}(\bar{\mathbf{f}})$ is invertible, we can express the condition (25) as

$$\mathbf{\Omega}^{-1}(\bar{\mathbf{f}})\mathbf{\Psi}(\bar{\mathbf{f}})\bar{\mathbf{f}} = \lambda(\bar{\mathbf{f}})\bar{\mathbf{f}}. \tag{29}$$

Regarding $\bar{\mathbf{f}}$ as an eigenvector and $\lambda(\bar{\mathbf{f}})$ as a corresponding eigenvalue of $\mathbf{\Omega}^{-1}(\bar{\mathbf{f}})\mathbf{\Psi}(\bar{\mathbf{f}})$, the first-order optimality condition (25) is same as a functional eigenvalue problem, i.e., (25) is cast as a NEPv [22]. To find the stationary point that maximizes the objective function, we need to find $(\bar{\mathbf{f}}^\dagger, \mu^\dagger)$ which maximizes $\lambda(\bar{\mathbf{f}}^\dagger)$. Accordingly, we find the principal eigenvector of (29), $\bar{\mathbf{f}}^\star$, with corresponding $\mu^\star$ that satisfies the SCNR constraint and maximizing $\lambda(\bar{\mathbf{f}})$. Then computed $\bar{\mathbf{f}}^\star$ is expected to be the best stationary point. The following proposition summarizes the observation:

Proposition 1. *Consider $\bar{\mathbf{f}}^\star$ as a principal eigenvector of $\mathbf{\Omega}^{-1}(\bar{\mathbf{f}}^\star)\mathbf{\Psi}(\bar{\mathbf{f}}^\star)$ satisfying*

$$\mathbf{\Omega}^{-1}(\bar{\mathbf{f}}^\star)\mathbf{\Psi}(\bar{\mathbf{f}}^\star)\bar{\mathbf{f}}^\star = \lambda(\bar{\mathbf{f}}^\star)\bar{\mathbf{f}}^\star \tag{30}$$

with corresponding $\mu^\star$ where $(\bar{\mathbf{f}}^\star, \mu^\star)$ satisfy the SCNR constraint (24)*. Then $\bar{\mathbf{f}}^\star$ is the best stationary point of the problem* (23).

We introduce an efficient algorithm to iteratively compute the principal eigenvector from Proposition 1, named as GPI-based ISAC (GPI-ISAC). GPI-ISAC alternately computes $\bar{\mathbf{f}}$ for given μ and μ for given $\bar{\mathbf{f}}$ until it search $(\bar{\mathbf{f}}^\star, \mu^\star)$. Firstly, we explain the ISAC beamforming optimization method to find $\bar{\mathbf{f}}$ for given μ [23]. At the t-th iteration, we build the matrices $\mathbf{\Psi}(\bar{\mathbf{f}}_{(t-1)})$ and $\mathbf{\Omega}(\bar{\mathbf{f}}_{(t-1)})$ using (26) and (27) based on $\bar{\mathbf{f}}_{(t-1)}$. Next, we compute $\bar{\mathbf{f}}_{(t)}$ as

$$\bar{\mathbf{f}}_{(t)} \leftarrow \frac{\mathbf{\Omega}^{-1}(\bar{\mathbf{f}}_{(t-1)})\mathbf{\Psi}(\bar{\mathbf{f}}_{(t-1)})\bar{\mathbf{f}}_{(t-1)}}{\|\mathbf{\Omega}^{-1}(\bar{\mathbf{f}}_{(t-1)})\mathbf{\Psi}(\bar{\mathbf{f}}_{(t-1)})\bar{\mathbf{f}}_{(t-1)}\|}. \tag{31}$$

Until the convergence criteria $\left\|\bar{\mathbf{f}}_{(t)} - \bar{\mathbf{f}}_{(t-1)}\right\| < \epsilon$ for $\epsilon > 0$ satisfied, We repeat this process. After converge, the computed $\bar{\mathbf{f}}$ is the principal eigenvector of $\mathbf{\Omega}^{-1}(\bar{\mathbf{f}})\mathbf{\Psi}(\bar{\mathbf{f}})$. The overall process is summarized in Algorithm 1.

Now we attempt to find the desired Lagrangian multiplier μ for a given $\bar{\mathbf{f}}$. In the Lagrangian function (41), the Lagrangian multiplier μ balances maximizing the objective function and activating the SCNR constraint. For large μ, the optimization process pursues to increase the receive SCNR, to meet the constraint. In this scenario, the objective function, specifically the sum SE, is not maximized efficiently. For small μ, the optimization process pursues to maximize the objective function, while being less interested in the SCNR constraint. Accordingly, to maximize the objective function effectively while fulfilling the SCNR constraint, μ should be found as a proper value.

To find proper μ, we adopt a binary search-based algorithm. We set the minimum and maximum values of μ as $\mu_{\min}$ and $\mu_{\max}$. After we fine a stationary point $\bar{\mathbf{f}}$ for given μ, we verify if $T_{\text{scnr}} < \mathrm{Tr}\left(\mathbf{G}_{\text{tar}}\mathbf{F}\mathbf{F}^{\mathsf{H}}\mathbf{G}_{\text{tar}}^{\mathsf{H}}\right) / \left(\mathrm{Tr}\left(\mathbf{G}_{\text{cl}}\mathbf{F}\mathbf{F}^{\mathsf{H}}\mathbf{G}_{\text{cl}}^{\mathsf{H}}\right) + \frac{N}{P}\sigma_{\text{R}}^2\right)$. If this condition is met, we update μ smaller to search further the stationary point with less SCNR penalty, i.e., increase the weight on the objective function. Specifically, we decrease μ by $\mu \leftarrow (\mu + \mu_{\min})/2$ for such a case. On the contrary, if $T_{\text{scnr}} > \mathrm{Tr}\left(\mathbf{G}_{\text{tar}}\mathbf{F}\mathbf{F}^{\mathsf{H}}\mathbf{G}_{\text{tar}}^{\mathsf{H}}\right) / \left(\mathrm{Tr}\left(\mathbf{G}_{\text{cl}}\mathbf{F}\mathbf{F}^{\mathsf{H}}\mathbf{G}_{\text{cl}}^{\mathsf{H}}\right) + \frac{N}{P}\sigma_{\text{R}}^2\right)$, we increase μ as $\mu \leftarrow (\mu + \mu_{\max})/2$. Then we repeat Algorithm 1 with the updated μ. Until a convergence condition $|\mu_{(n)} - \mu_{(n-1)}| < \zeta$ is satisfied for $\zeta > 0$, we repeat this process. When the problem (23) is feasible, we can compute the smallest μ that meets the SCNR requirement, and find the solution $(\bar{\mathbf{f}}^\star, \mu^\star)$ in Proposition 1. We summarize the overall optimization process in Algorithm 2.

1) Extension to Radar-Only Setup: We explain the proposed optimization framework can be transformed into a radar-only setup. In a radar-only setup, a main target is maximizing the SCNR in (8). Then, the SCNR maximizing problem is formulated as

$$\underset{\bar{\mathbf{f}}}{\text{maximize}} \quad \gamma_{\mathrm{R}} = \frac{\operatorname{Tr}\left(\mathbf{G}_{\mathrm{tar}}\mathbf{F}\mathbf{F}^{\mathsf{H}}\mathbf{G}_{\mathrm{tar}}^{\mathsf{H}}\right)}{\operatorname{Tr}\left(\mathbf{G}_{\mathrm{cl}}\mathbf{F}\mathbf{F}^{\mathsf{H}}\mathbf{G}_{\mathrm{cl}}^{\mathsf{H}}\right) + \frac{N}{P}\sigma_{\mathrm{R}}^2} \tag{32}$$

$$\text{subject to} \quad \|\bar{\mathbf{f}}\|^2 \leq 1. \tag{33}$$

Through a similar process, the following corollary shows the stationarity condition of (32):

Corollary 1. *The optimal solution for the problem* (32) *is the principal eigenvector of the following generalized eigenvalue problem:*

$$\mathbf{\Omega}_{\mathrm{R}}^{-1}(\bar{\mathbf{f}})\mathbf{\Psi}_{\mathrm{R}}(\bar{\mathbf{f}})\bar{\mathbf{f}} = \lambda_{\mathrm{R}}(\bar{\mathbf{f}})\bar{\mathbf{f}}, \tag{34}$$

where $\mathbf{\Psi}_{\mathrm{R}} = \bar{\mathbf{G}}_{\mathrm{tar}}$ *in* (21) *and* $\mathbf{\Omega}_{\mathrm{R}} = \bar{\mathbf{G}}_{\mathrm{cl}}$ *in* (22).

Proof. Consider $\|\bar{\mathbf{f}}\|^2 = 1$, i.e., maximum transmit power. By the similar reformulation as Lemma 1, we rewrite the SCNR as

$$\gamma_{\mathrm{R}} = \frac{\bar{\mathbf{f}}^{\mathsf{H}}\bar{\mathbf{G}}_{\mathrm{tar}}\bar{\mathbf{f}}}{\bar{\mathbf{f}}^{\mathsf{H}}\bar{\mathbf{G}}_{\mathrm{cl}}\bar{\mathbf{f}}}, \tag{35}$$

which is a generalized Rayleigh quotient. Because $\|\bar{\mathbf{f}}\|^2 = 1$ is inherently excluded due to scaling invariance, the optimal solution is the principal eigenvector of $\bar{\mathbf{G}}_{\mathrm{cl}}^{-1}\bar{\mathbf{G}}_{\mathrm{tar}}$. ■

To find the principal eigenvector of (34) from Corollary 1, Algorithm 1 can be applied to a GPI-based radar beamforming algorithm with using $\mathbf{\Psi}_{\mathrm{R}}$ and $\mathbf{\Omega}_{\mathrm{R}}$ instead of $\mathbf{\Psi}$ and $\mathbf{\Omega}$, respectively.

IV. Numerical Results

In this section, we assess the performance of the proposed methods compared to existing benchmarks. Through the simulations, the number of angular sampling grids is set to $L = 256$ between $-\pi/2$ and $\pi/2$ in radians. we use the channel model in [24], to construct the channel and its covariance matrix $\mathbf{K}_k$. The channel estimation quality parameter is $\kappa = 0.3$. We consider $\mu_{\min} = 0$ and $\mu_{\max} = 2000$ for proposed algorithm. Furthermore, we set all convergence thresholds as 10^{-3} and maximum iteration counts as 20. We also define $\mathrm{SNR} = P/\sigma^2$. We assume a uniform linear array (ULA) antenna in the simulations.

For the channels, we consider frequency division duplex (FDD) systems. $\hat{\mathbf{h}}_k$ is described in [25] as

$$\hat{\mathbf{h}}_k = \mathbf{U}_k\mathbf{\Lambda}_k^{\frac{1}{2}}\left(\sqrt{1-\kappa^2}\tilde{\mathbf{h}}_k + \kappa\mathbf{v}_k\right) = \sqrt{1-\kappa^2}\mathbf{h}_k + \mathbf{q}_k, \tag{36}$$

where $\mathbf{v}_k \sim \mathcal{CN}(\mathbf{0}_{N\times 1}, \mathbf{I}_N)$, $\mathbf{q}_k$ is the CSIT quantization error and $\kappa \in [0,1]$ is a channel quality parameter. In particular, the channel estimation error covariance matrix is $\mathbf{\Phi}_k = \mathbf{U}_k\mathbf{\Lambda}_k^{\frac{1}{2}}(2 - 2\sqrt{1-\kappa^2})\mathbf{\Lambda}_k^{\frac{1}{2}}\mathbf{U}_k^{\mathsf{H}}$.

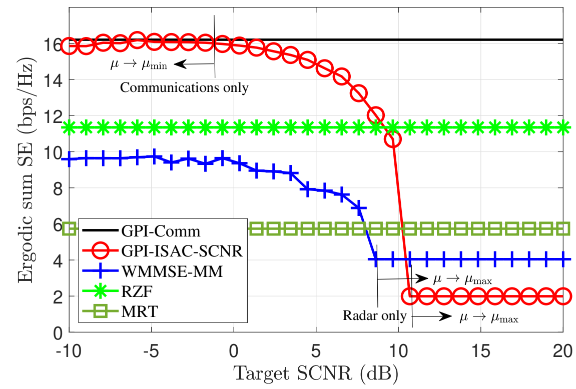

(a) Achieved SE

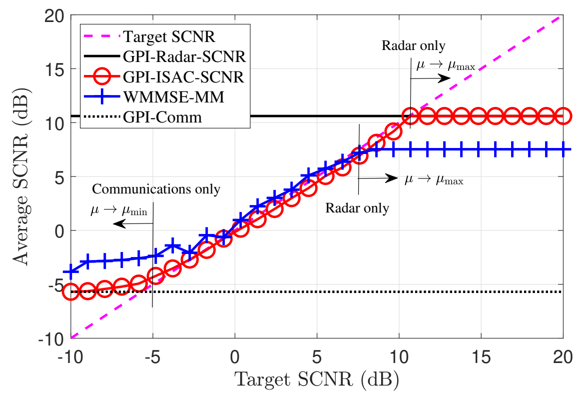

(b) Achieved SCNR

Fig. 1. (a) The ergodic sum SE and (b) the average SCNR versus target SCNR for $N = 8$, $K = 4$, $M = 8$, and 20 dB SNR.

Now, we concisely explain the conventional approach to solving optimization problems in ISAC systems as a benchmark. Based on the WMMSE-MM algorithm in [16], the optimization problem is solved as follows:

$$\underset{\mathbf{F}}{\text{maximize}} \quad \sum_{k=1}^{K} R_k + \mu\mathbf{a}^{\mathsf{H}}(\theta^*)\mathbf{F}\mathbf{F}^{\mathsf{H}}\mathbf{a}(\theta^*) \tag{37}$$

$$\text{subject to} \quad \|\mathbf{F}\|_{\mathsf{F}} = 1, \tag{38}$$

where θ^* is the intended radar beam angle. For reference, we employ our binary tree search-based method to find μ that the computed $\mathbf{F}$ meets the SCNR constraint as same as the problem in (9). Then, the following communication and radar performance are assessed as a benchmark for GPI-ISAC-SCNR for single-target and multi-target cases.

In Fig. 1, we plot the ergodic sum SE and the achieved SCNR performance. The simulation results demonstrate that GPI-ISAC-SCNR significantly outperforms WMMSE-MM and linear precoders such as regularized zero-forcing (RZF) and maximum ratio transmission (MRT) in terms of sum SE across the feasible target SCNR range. At lower target SCNR, the sum SE of GPI-ISAC-SCNR and WMMSE-MM stabilizes at different levels. Notably, the performance gap in terms of the sum SE between GPI-ISAC-SCNR and GPI-Comm decreases as the target SCNR decreases. This convergence occurs when

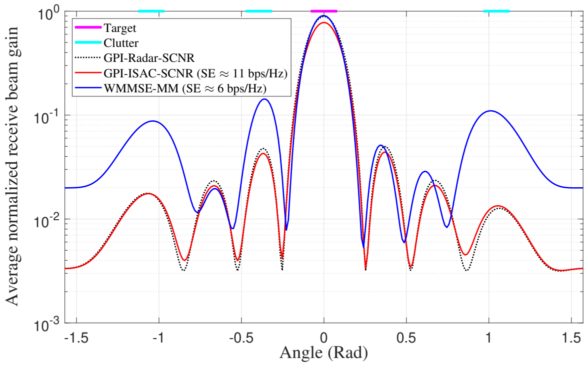

Fig. 2. Normalized receive beam patterns of the GPI-based methods and WMMSE-MM, with achieved sum SEs of approximately 11 bps/Hz for GPI-ISAC-SCNR and 6 bps/Hz for WMMSE-MM.

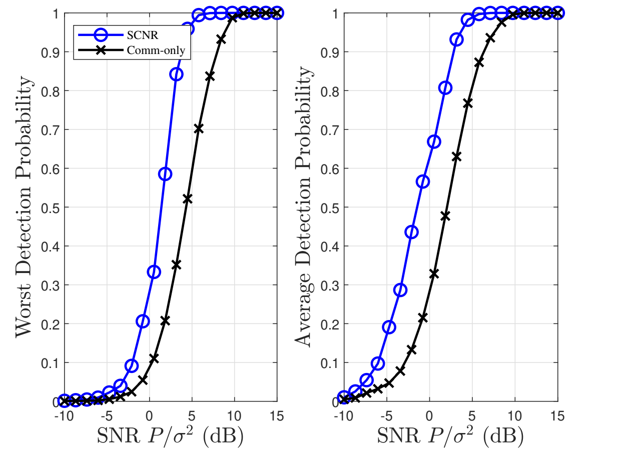

Fig. 3. The detection probability for multi-target cases with $N = 8, K = 4$, and $M = 8$.

the target SCNR falls below achieved SCNR of GPI-Comm, allowing the target SCNR to be met with $\mu = 0$. Conversely, the GPI-ISAC-SCNR and WMMSE-MM algorithms exhibit a sharp decline in the sum SE beyond a certain target SCNR, as they concentrate resources to maximize SCNR, i.e., $\mu \longrightarrow \mu_{\max}$. This substantial drop of the performance is evident when the algorithms fail to meet the target SCNR (> 11 dB), as shown in Fig. 1(b). In the presence of clutters, GPI-ISAC-SCNR offers a wider feasible target SCNR range compared to WMMSE-MM. Consequently, GPI-ISAC-SCNR shows more suitable than WMMSE-MM when dealing with significant clutter interference.

Fig. 2 presents a normalized receive beam gain through the angular grid. The normalized receive beam gain for θ_ℓ is calculated as:

$$\frac{1}{P}\mathbb{E}[|\mathbf{a}_{\mathrm{r}}^{\mathsf{H}}(\theta_\ell)\mathbf{y}_{\mathrm{R}}|^2] = \mathbf{a}_{\mathrm{r}}^{\mathsf{H}}\left(\mathbf{G}\mathbf{F}\mathbf{F}^{\mathsf{H}}\mathbf{G}^{\mathsf{H}} + \frac{\sigma_{\mathrm{R}}^2}{P}\mathbf{I}_N\right)\mathbf{a}_{\mathrm{r}}, \tag{39}$$

where $\mathbf{G} = \mathbf{G}_{\mathrm{tar}} + \mathbf{G}_{\mathrm{cl}}$. The attained sum SE is approximately 11 bps/Hz for GPI-ISAC-SCNR and 6 bps/Hz for WMMSE-MM. Despite achieving the higher sum SE, GPI-ISAC-SCNR exhibits a superior receive beam pattern compared to WMMSE-MM. It provides a comparable main lobe for the target angle while producing significantly lower side lobes. The achieved SCNR for GPI-ISAC-SCNR is approximately 11 dB, while WMMSE-MM achieves approximately 6 dB. In this regard, the proposed algorithm surpasses WMMSE-MM with respect to beam design accuracy and the SE.

We present a quantitative analysis of radar metric such as SCNR. This analysis is performed by evaluating the detection probability of our proposed algorithm. For comparison, we also evaluate the proposed algorithm in the communication-only case. For the evaluation, we set $N = 8$, $K = 4$, and $M = 8$. Then, the reflection coefficients of the targets and clutters are set as $|\beta_i^{\mathrm{tar}}| = 1$ and $|\beta_i^{\mathrm{cl}}| = 10, \forall i$, respectively. We maintain a target probability of false alarm at 10^{-4}. In Fig. 3, we illustrate the detection probability for multi-target cases as a function of transmit SNR. We position the target at an angle of $-\pi/4, 0, \pi/3$ radians, with cluttering angles at $-\pi/3, \pi/8$ radians. As shown in Fig. 3, we demonstrate that the proposed algorithm achieves comparable detection probabilities in terms of worst detection and average detection probability than the comm-only algorithm. Since the proposed algorithm accounts for cluttering during beamforming optimization, it can achieve higher performance than the comm-only algorithm. Therefore, the proposed algorithm demonstrates robust detection capabilities in cluttered environments, effectively considering SCNR in optimization.

V. Conclusion

In this paper, we proposed a comprehensive beamforming framework for ISAC systems considering imperfect CSIT. By utilizing the SCNR metric for a radar constraint, we developed a communication-focused problem aimed at maximizing the sum SE while fulfilling the SCNR constraint. Firstly, we reformulated the problem into a vectorized joint beamformer format to address this issue and derived the KKT stationarity condition. regarding the condition as a functional eigenvalue problem, we employed the GPI algorithm to find the best stationary point. Simulation results proved that the proposed GPI-ISAC-SCNR algorithms outperformed the state-of-the-art ISAC algorithms in both communication and radar performance with imperfect CSIT. In conclusion, the proposed ISAC beamforming framework is powerful, making it applicable to ISAC scenarios while ensuring high efficiency in communication and radar applications.

VI. Acknowledgement

This research was supported by the MSIT(Ministry of Science and ICT), Korea, under the ITRC(Information Technology Research Center) support program(IITP-2023-RS-2023-00259991) supervised by the IITP(Institute for Information & Communications Technology Planning & Evaluation)"

Appendix A
Proof of Lemma 1

Here, we transform the SCNR constraint to a log function to make a scalable constraint of the sum SE as

$$\log_2\left(\frac{\bar{\mathbf{f}}^{\mathsf{H}}\bar{\mathbf{G}}_{\text{tar}}\bar{\mathbf{f}}}{\bar{\mathbf{f}}^{\mathsf{H}}\bar{\mathbf{G}}_{\text{cl}}\bar{\mathbf{f}}}\right) \geq \log_2 T_{\text{scnr}}. \tag{40}$$

The Lagrangian function of (23) with (40) is

$$\begin{aligned}\tilde{L}(\bar{\mathbf{f}};\mu) &= \log_2 \prod_{k=1}^{K}\left(\frac{\bar{\mathbf{f}}^{\mathsf{H}}\mathbf{B}_k\bar{\mathbf{f}}}{\bar{\mathbf{f}}^{\mathsf{H}}\mathbf{C}_k\bar{\mathbf{f}}}\right) + \mu\left(\log_2\left(\frac{\bar{\mathbf{f}}^{\mathsf{H}}\bar{\mathbf{G}}_{\text{tar}}\bar{\mathbf{f}}}{\bar{\mathbf{f}}^{\mathsf{H}}\bar{\mathbf{G}}_{\text{cl}}\bar{\mathbf{f}}}\right) - \log_2 T_{\text{scnr}}\right)\\ &= \log_2 \lambda(\bar{\mathbf{f}}). \end{aligned} \tag{41}$$

Then, the stationarity condition requires

$$\frac{\partial \tilde{L}(\bar{\mathbf{f}},\mu)}{\partial \bar{\mathbf{f}}} = \frac{\partial \tilde{L}(\bar{\mathbf{f}},\mu)}{\partial \lambda(\bar{\mathbf{f}})}\frac{\partial \lambda(\bar{\mathbf{f}})}{\partial \bar{\mathbf{f}}} = \frac{1}{\lambda(\bar{\mathbf{f}})\log 2}\frac{\partial \lambda(\bar{\mathbf{f}})}{\partial \bar{\mathbf{f}}} = 0. \tag{42}$$

Therefore, we derive the condition for $\frac{\partial \lambda(\bar{\mathbf{f}})}{\partial \bar{\mathbf{f}}} = 0$ which is same as (42).

$$\begin{aligned}\frac{\partial \lambda(\bar{\mathbf{f}})}{\partial \bar{\mathbf{f}}} &= 2\lambda(\bar{\mathbf{f}})\left[\sum_{k=1}^{K}\left(\frac{\mathbf{B}_k\bar{\mathbf{f}}}{\bar{\mathbf{f}}^{\mathsf{H}}\mathbf{B}_k\bar{\mathbf{f}}} - \frac{\mathbf{C}_k\bar{\mathbf{f}}}{\bar{\mathbf{f}}^{\mathsf{H}}\mathbf{C}_k\bar{\mathbf{f}}}\right) + \mu\left(\frac{\bar{\mathbf{G}}_{\text{tar}}\bar{\mathbf{f}}}{\bar{\mathbf{f}}^{\mathsf{H}}\bar{\mathbf{G}}_{\text{tar}}\bar{\mathbf{f}}} - \frac{\bar{\mathbf{G}}_{\text{cl}}\bar{\mathbf{f}}}{\bar{\mathbf{f}}^{\mathsf{H}}\bar{\mathbf{G}}_{\text{cl}}\bar{\mathbf{f}}}\right)\right]\\ &= 0. \end{aligned} \tag{43}$$

By rearranging the condition in (43), we have

$$\lambda_{\mathsf{num}}(\bar{\mathbf{f}})\left(\sum_{k=1}^{K}\frac{\mathbf{B}_k}{\bar{\mathbf{f}}^{\mathsf{H}}\mathbf{B}_k\bar{\mathbf{f}}} + \mu\frac{\bar{\mathbf{G}}_{\text{tar}}}{\bar{\mathbf{f}}^{\mathsf{H}}\bar{\mathbf{G}}_{\text{tar}}\bar{\mathbf{f}}}\right)\bar{\mathbf{f}} \tag{44}$$

$$= \lambda_{\mathsf{den}}(\bar{\mathbf{f}})\left(\sum_{k=1}^{K}\frac{\mathbf{C}_k}{\bar{\mathbf{f}}^{\mathsf{H}}\mathbf{C}_k\bar{\mathbf{f}}} + \mu\frac{\bar{\mathbf{G}}_{\text{cl}}}{\bar{\mathbf{f}}^{\mathsf{H}}\bar{\mathbf{G}}_{\text{cl}}\bar{\mathbf{f}}}\right)\lambda(\bar{\mathbf{f}})\bar{\mathbf{f}}. \tag{45}$$

This completes the proof. ■

References

[1] W. Saad, M. Bennis, and M. Chen, "A vision of 6g wireless systems: Applications, trends, technologies, and open research problems," *IEEE network*, vol. 34, no. 3, pp. 134–142, 2019.

[2] F. Liu, Y. Cui, C. Masouros, J. Xu, T. X. Han, Y. C. Eldar, and S. Buzzi, "Integrated sensing and communications: Toward dual-functional wireless networks for 6g and beyond," *IEEE journal on selected areas in communications*, vol. 40, no. 6, pp. 1728–1767, 2022.

[3] F. Liu, C. Masouros, A. P. Petropulu, H. Griffiths, and L. Hanzo, "Joint radar and communication design: Applications, state-of-the-art, and the road ahead," *IEEE Transactions on Communications*, vol. 68, no. 6, pp. 3834–3862, 2020.

[4] M. L. Rahman, J. A. Zhang, X. Huang, Y. J. Guo, and R. W. Heath, "Framework for a perceptive mobile network using joint communication and radar sensing," *IEEE Transactions on Aerospace and Electronic Systems*, vol. 56, no. 3, pp. 1926–1941, 2019.

[5] H. Que, J. Yang, C.-K. Wen, S. Xia, X. Li, and S. Jin, "Joint beam management and slam for mmwave communication systems," *IEEE Transactions on Communications*, 2023.

[6] C. Sturm and W. Wiesbeck, "Waveform design and signal processing aspects for fusion of wireless communications and radar sensing," *Proceedings of the IEEE*, vol. 99, no. 7, pp. 1236–1259, 2011.

[7] A. R. Chiriyath, B. Paul, G. M. Jacyna, and D. W. Bliss, "Inner bounds on performance of radar and communications co-existence," *IEEE Transactions on Signal Processing*, vol. 64, no. 2, pp. 464–474, 2015.

[8] Y. Liu, G. Liao, J. Xu, Z. Yang, and Y. Zhang, "Adaptive ofdm integrated radar and communications waveform design based on information theory," *IEEE Communications Letters*, vol. 21, no. 10, pp. 2174–2177, 2017.

[9] M. F. Keskin, V. Koivunen, and H. Wymeersch, "Limited feedforward waveform design for ofdm dual-functional radar-communications," *IEEE Transactions on Signal Processing*, vol. 69, pp. 2955–2970, 2021.

[10] A. Hassanien, M. G. Amin, Y. D. Zhang, and F. Ahmad, "Dual-function radar-communications: Information embedding using sidelobe control and waveform diversity," *IEEE Transactions on Signal Processing*, vol. 64, no. 8, pp. 2168–2181, 2015.

[11] D. Ma, N. Shlezinger, T. Huang, Y. Liu, and Y. C. Eldar, "Frac: Fmcw-based joint radar-communications system via index modulation," *IEEE journal of selected topics in signal processing*, vol. 15, no. 6, pp. 1348–1364, 2021.

[12] F. Liu, C. Masouros, A. Li, H. Sun, and L. Hanzo, "Mu-mimo communications with mimo radar: From co-existence to joint transmission," *IEEE Transactions on Wireless Communications*, vol. 17, no. 4, pp. 2755–2770, 2018.

[13] F. Liu, L. Zhou, C. Masouros, A. Li, W. Luo, and A. Petropulu, "Toward dual-functional radar-communication systems: Optimal waveform design," *IEEE Transactions on Signal Processing*, vol. 66, no. 16, pp. 4264–4279, 2018.

[14] H. Hua, J. Xu, and T. X. Han, "Optimal transmit beamforming for integrated sensing and communication," *IEEE Transactions on Vehicular Technology*, vol. 72, no. 8, pp. 10 588–10 603, 2023.

[15] X. Liu, T. Huang, N. Shlezinger, Y. Liu, J. Zhou, and Y. C. Eldar, "Joint transmit beamforming for multiuser mimo communications and mimo radar," *IEEE Transactions on Signal Processing*, vol. 68, pp. 3929–3944, 2020.

[16] C. Xu, B. Clerckx, and J. Zhang, "Multi-antenna joint radar and communications: Precoder optimization and weighted sum-rate vs probing power tradeoff," *IEEE Access*, vol. 8, pp. 173 974–173 982, 2020.

[17] N. Su, F. Liu, and C. Masouros, "Secure radar-communication systems with malicious targets: Integrating radar, communications and jamming functionalities," *IEEE Transactions on Wireless Communications*, vol. 20, no. 1, pp. 83–95, 2020.

[18] Z. Ren, L. Qiu, J. Xu, and D. W. K. Ng, "Robust transmit beamforming for secure integrated sensing and communication," *IEEE Transactions on Communications*, vol. 71, no. 9, pp. 5549–5564, 2023.

[19] G. Cui, H. Li, and M. Rangaswamy, "Mimo radar waveform design with constant modulus and similarity constraints," *IEEE Transactions on signal processing*, vol. 62, no. 2, pp. 343–353, 2013.

[20] H. Joudeh and B. Clerckx, "Sum-rate maximization for linearly precoded downlink multiuser miso systems with partial csit: A rate-splitting approach," *IEEE Transactions on Communications*, vol. 64, no. 11, pp. 4847–4861, 2016.

[21] M. Ding and S. D. Blostein, "Maximum mutual information design for mimo systems with imperfect channel knowledge," *IEEE transactions on information theory*, vol. 56, no. 10, pp. 4793–4801, 2010.

[22] Y. Cai, L.-H. Zhang, Z. Bai, and R.-C. Li, "On an eigenvector-dependent nonlinear eigenvalue problem," *SIAM Journal on Matrix Analysis and Applications*, vol. 39, no. 3, pp. 1360–1382, 2018.

[23] J. Choi, N. Lee, S.-N. Hong, and G. Caire, "Joint user selection, power allocation, and precoding design with imperfect csit for multi-cell mu-mimo downlink systems," *IEEE Transactions on Wireless Communications*, vol. 19, no. 1, pp. 162–176, 2019.

[24] A. Adhikary, J. Nam, J.-Y. Ahn, and G. Caire, "Joint spatial division and multiplexing—the large-scale array regime," *IEEE transactions on information theory*, vol. 59, no. 10, pp. 6441–6463, 2013.

[25] J. Park, N. Lee, J. G. Andrews, and R. W. Heath, "On the optimal feedback rate in interference-limited multi-antenna cellular systems," *IEEE Transactions on Wireless Communications*, vol. 15, no. 8, pp. 5748–5762, 2016.